

A Numerical Test of Air-Void Spacing Equations

Kenneth A. Snyder

National Institute of Standards and Technology

Building Materials Division

Gaithersburg, MD 20899

January 2, 1998

Abstract

Air void spacing equations have been proposed in the literature by a number of authors: Powers; Philleo; Attiogbe; and Pleau and Pigeon. Each proposed spacing equation attempts to characterize the true “spacing” of entrained air voids in concrete. While efforts have been made to correlate these spacing equation calculations to freeze-thaw performance, no test has been performed to assess the geometrical accuracy of these spacing equations. Herein is a computerized accuracy test of these proposed spacing equations. A computer model of air void systems is used, and various “spacings” are measured in the model system. The results of these measurements are then compared to the appropriate spacing equation prediction, along with equations developed by Lu and Torquato.

Keywords: entrained air voids; concrete; freeze-thaw; spacing equations

1 Introduction

The efficacy of entrained air voids in concrete for providing freeze-thaw durability has been known since the 1940's [1]. However, their exact role in freeze-thaw durability has not been established definitively. There appears to be a connection between the expansion of the water during freezing and the proximity of the air voids. Regardless of which particular physical theory of freeze-thaw degradation might be correct, an undisputed fact is that good freeze-thaw durability can be achieved through the presence of many small entrained air voids distributed throughout the cement paste phase of the concrete. Therefore, one could characterize an air void system by estimating some measure of air void "spacing," with the expectation that concretes with equal air contents, but different air void spacings, should exhibit different freeze-thaw performance.

One of the first attempts to characterize the "spacing" of air voids was by Powers [2], which was the basis for the American Society for Testing and Materials (ASTM) C 457 [3] spacing factor (\bar{L}). Since then, spacing equations have been proposed by Philleo [4], Attiogbe [5], and Pleau and Pigeon [6]. Each of these equations attempts to characterize the "spacing" of voids in air-entrained concrete, even though the Attiogbe equation estimates the spacing among air voids, and the other equations estimate the distance water must travel to reach the nearest air void.

At present, evaluation of an air void spacing equation consists of a comparison between the estimation of spacing and the results of laboratory freeze-thaw experiments [7, 8]. The *a priori* assumption is that each equation is inherently correct in its estimation of spacing. Unfortunately, each of these spacing equations proposed for predicting freeze-thaw performance has inherent assumptions or simplifications built into its development. Until now, no quantitative measure has been made of the effects due to these assumptions.

This paper quantifies the performance of the various spacing equations using a computerized numerical experiment. The computer experiment measures various "spacing"

quantities in a paste-air system. Systems are composed of air voids with either mono-sized or lognormally distributed radii. Since the size and the location of each sphere are known exactly, the actual “spacings” can also be calculated exactly. To achieve acceptable statistics, the results from many system realizations are used to estimate averaged quantities. These results, along with the associated spacing equation predictions, are reported for comparison.

2 Spacing Distributions

There are two classifications of spacing equations which will be discussed here. Some equations estimate the proximity of the paste to the voids, and others estimate the proximity of the voids to one another. Although this may seem a subtle distinction, it will be shown that the mathematical relationships that characterize these concepts have different behaviors.

Also, any reasonable concept of “spacing” should address the fact that there must exist a distribution of distances which characterize the spacing. Clearly, some regions of the paste are closer to an air void than other regions, and some voids have nearer neighbors than others. This characteristic can be represented by a distribution of distances, as depicted in Fig. 1 for a distance s . In this figure, the probability density function (PDF) is a normalized function with unit area under its curve. This function represents the fraction of spacings found in the interval $[s, s + ds]$ for some differential element ds . The associated cumulative distribution function (CDF) is the integral of the PDF. This function increases monotonically from zero to unity and represents the fraction of spacings less than s .

An illustration of using the CDF is also shown in Fig. 1. Two horizontal dashed lines intercept the ordinate axis at the 50 *th* and 95 *th* percentiles. These lines intercept the CDF at s values of 1.95 and 3.1, respectively. Therefore, 50 % of the spacings are less than 1.95, and 95 % are less than 3.1. In theory, the CDF only asymptotes to unity, and to capture all of the spacings, s must increase to infinity. In practice, however,

the quantity s can only increase to the size of the system. Therefore, the concept of a maximum spacing is an ill-defined quantity. Therefore, in this experiment, the 50 *th* and the 95 *th* percentiles of the spacing distributions will be used to characterize both the measured and the estimated values.

2.1 Analytical Equations-Discrete Data

This numerical experiment is performed by collecting a finite number of spacing values and comparing this distribution of spacings to an analytic equation. The most straightforward way to do this is to use all of the data to create a discrete cumulative distribution function for the data, and compare percentiles of this function to the same percentiles computed for the analytic equations. As a simple demonstration of this procedure, 20 normally distributed random numbers with a mean of zero and a variance of one were generated by a computer program [9] and sorted from smallest to largest. These data, labeled x , are shown in the first column of Table 1. The adjacent column contains the rank of the sorted x values. A rank of 10 signifies that 10 of the 20 values are less than x . The percentiles of the x values are calculated by dividing the rank by the total number of variates, 20. This percentile, or relative rank, is labeled y and is shown in the last column of the table. This value represents the numerically determined CDF of the x values, and is plotted in Fig. 2. Since the normal distribution is symmetric about zero, both the mean and 50 *th* percentile are also zero. From Table 1, the 50 *th* percentile of the data is approximately -0.104, which differs from the true value of zero. The error is due to the small sample size. Repeating this experiment of 20 random variates and averaging the results would yield a more accurate estimate of the 50 *th* percentile.

Another way to increase accuracy is to increase the number of random numbers. Fig. 3 shows the CDF created from a single experiment of 1000 normally distributed random deviates, again with mean zero and variance one. From these data, one could either estimate percentiles of the distribution, or estimate the PDF of the data. The 50 *th* percentile of the discrete CDF is 0.018, which is a more accurate estimate than

for the 20 variates. An estimate of the PDF for these data was calculated by first extracting every 40 *th* value in the CDF data in order to reduce noise in the data. A one-sided finite difference [10] algorithm was used to calculate the slope at these points (the derivative of the CDF) and these values for the probability density function (PDF) are shown as filled circles in Fig. 3. For a comparison, the true gaussian PDF is also shown in the figure. Even after smoothing the CDF by selecting every 40 *th* value, the resulting PDF is still quite noisy. Therefore, a comparison between measured data and analytic estimates is best done through estimating percentiles using the CDF.

2.2 Paste-Void Proximity

Paste-void proximity equations estimate the volume fraction of paste within some distance from the surface of the nearest air void. There are two simple ways to visualize this spacing: (1) Imagine surrounding each air void with a shell of thickness s . These shells may overlap one another, but may not overlap or penetrate air voids. The volume fraction of the paste that is within any shell is equivalent to the volume fraction of paste within a distance s of an air void surface. (2) Given an air void system, pick points at random throughout the paste which lie outside the air voids. For each point, find the distance to the nearest air void surface. The number fraction of the points that fall within a distance s of an air void surface is equal to the volume fraction of paste within a distance s of an air void surface. This second approach is the one used here to estimate the CDF of the spacing distribution.

This definition of the paste-void proximity distribution is the same as that used by proponents of the protected paste volume (PPV) concept [11–13]. The material parameters of the concrete determine the limiting spacing, and one wants to determine the fraction of paste within this distance to the nearest air void.

2.3 Void-Void Proximity

Void-void proximity spacing equations can be further classified into either nearest neighbor or mean free path calculations.

2.3.1 Nearest Neighbor

Nearest neighbor void-void proximity equations estimate the surface-surface distance between nearest neighbor air voids. This is calculated by starting from a given air void and finding the shortest distance from the surface of that void to the surface of any other air void. This is repeated for a number of different air voids. This collection of random distances, when sorted and plotted versus its relative rank, form an estimated void-void proximity cumulative distribution function.

As will be demonstrated subsequently, void-void proximity spacings have a subtle complexity. For an air-void system composed of polydispersed sphere diameters, the average void-void spacing originating from large spheres is smaller than the average void-void spacing originating from small spheres. Therefore, the “mean void-void spacing” is an ill-defined quantity when stated without additional qualifiers, since it varies over the distribution of sphere diameters.

2.3.2 Mean Free Path

The mean free path is the average length of paste between adjacent air voids along a randomly chosen line passing through the air void system. If an ASTM C 457 [3] linear traverse was performed on a paste specimen containing entrained air voids, the mean free path would be equal to the average paste chord length. It is important to note that this distance is neither the longest nor the shortest distance between air voids in an air void system.

An important difference between the mean free path and either the void-void or the paste-void proximity spacings is that the mean free path is simply a number, and not a distribution. The advantage is that a single number can be used to characterize this

measure of spacing. The disadvantage is that a single number yields no information about the expected variability

n : number of air voids per unit volume.

A : air void volume fraction.

p : paste volume fraction.

α : specific surface area of spheres.

r : sphere radii.

$f(r)$: sphere radii probability density function.

$\langle R^k \rangle$: the expected value of R^k for the radius distribution.

s : spacing distribution parameter.

For the paste-air systems (no aggregate) considered here, these quantities can be defined analytically as follows [15, 16]:

$$A \equiv \frac{4\pi}{3}n\langle R^3 \rangle \quad (1)$$

$$p \equiv 1 - A \quad (2)$$

$$\alpha \equiv \frac{4\pi n\langle R^2 \rangle}{\frac{4\pi n}{3}\langle R^3 \rangle} \quad (3)$$

$$\langle R^k \rangle \equiv \int_0^\infty r^k f(r) dr \quad (4)$$

The distinction has been made between the random variable R and its possible values r (see Ref. [16], Chapter 4).

4.1 Powers Spacing Factor

The most widely used paste-void spacing equation is the Powers spacing factor [2]. Contrary to a popular misconception, it does not attempt to estimate the distance between air voids. Rather, it is an attempt to calculate the fraction of paste within some distance of an air void (paste-void proximity). The Powers equation *approximates* the distance from the surface of all the air void surfaces which would encompass some large fraction of the paste. However, the value of this fraction is not quantified.

The second misconception is that the Powers spacing factor represents the maximum distance water must travel to reach the nearest air void in a concrete specimen [3, 8, 17]. From the previous discussion of the distribution of paste-void and void-void spacings, it should be clear that there is no single theoretical maximum value for the paste-void spacings. One can only quantify percentiles of the distribution to characterize the fraction of paste within some distance to the nearest air void surface. In practice, the maximum paste-void spacing is the size of the sample.

The Powers spacing factor was developed using two idealized systems. For small values of the p/A ratio, there is very little paste for each air void. Powers used the “frosting” approach of spreading all of the paste in a uniformly thick layer over each air void. The thickness of this “frosting” is approximately equal to the ratio of the volume of paste to the total surface area of air voids,

$$\bar{L} = \frac{p}{4\pi n\langle R^2 \rangle} = \frac{p}{\alpha A} \quad : p/A < 4.33 \quad (5)$$

For large values of the p/A ratio, Powers used the cubic lattice approach. The spheres are placed at the vertices of a simple cubic array. The air voids are monosized, each with a specific surface area equal to the bulk value. The cubic lattice spacing is chosen such that the air content equals the bulk value. The resulting Powers spacing factor is the distance from the center of a unit cell to the nearest air void surface,

$$\bar{L} = \frac{3}{\alpha} \left[1.4 \left(\frac{p}{A} + 1 \right)^{1/3} - 1 \right] \quad : p/A \geq 4.33 \quad (6)$$

The p/A value of 4.33 is the point at which these two equations are equal.

The intent was that a large fraction of the paste should be within \bar{L} of an air void surface. An acceptable value of \bar{L} for good freeze-thaw performance was determined from estimating material properties of concrete.

4.2 Philleo Spacing Equation

Philleo [4] extended the approach of Powers by attempting to quantify the volume fraction of paste within some distance of an air void system (paste-void proximity). Philleo started with an idealized air void system composed of randomly distributed points, the statistics of which are known. Using the Hertz [18] distribution for the paste-void proximity distribution for zero-radius points, Philleo then modified this distribution to account for finite sized spheres by renormalizing the cumulative distribution to account for the air content. The result, although still only an *approximation*, characterizes the paste-void spacings for finite-sized air voids. For an air-paste system, the Philleo spacing factor for the volume fraction of paste within a distance s of an air void surface is

$$F(s) = 1 - \exp \left[-4.19x^3 - 7.80x^2 [\ln(1/p)]^{1/3} - 4.84x [\ln(1/p)]^{2/3} \right] \quad (7)$$

where the substitution $x = sn^{1/3}$ has been made.

4.3 Attiogbe Spacing Equation

Recently, Attiogbe proposed a spacing equation which estimates the “mean spacing of air voids” in concrete [5]. From the author’s figures, it appears as though the Attiogbe spacing equation attempts to estimate one half the minimum surface-surface spacing among neighboring air voids. An accurate numerical test of the equation is complicated by the exact definition of what the author’s spacing equation attempts to quantify. Figure 1 of Ref. [5] depicts the “spacings” considered. In that figure, the author has chosen the nearest three voids as neighbors. The author should have included the other six voids that are “visible” to the central void since, by the author’s definition, “ \bar{d} is defined by considering only the distances, between adjacent air voids, which are entirely occupied by paste” [5].

A definitive numerical test of the Attiogbe [5] spacing equation is complicated further by the author’s ambiguous definitions of certain mathematical quantities. The author states both in the abstract and in the conclusion that the Attiogbe spacing

equation

$$t = 2 \frac{p^2}{\alpha A} \quad (8)$$

is, "... valid for all values of paste-to-air ratio, p/A " [5]. (To avoid confusion with the other spacing equations presented here, the variable t has been substituted for \bar{s} in the author's original equation.) When it was pointed out that for large values of p/A the equation diverges to infinity [19], the author revised the equation to

$$t_G = 2G p^2$$

accuracy [15]:

$$\lambda = \frac{p}{n\pi\langle R^2 \rangle} \quad (11)$$

If the center of the air voids remain fixed, as the radii of the air voids decreases to zero, the mean free path diverges toward infinity, like the Attiogbe equation for t .

This similarity is more than coincidental. In fact, the Attiogbe equation for t is directly proportional to λ . Expressing the Attiogbe equation for t as

$$t = 2p \frac{p}{\alpha A} \quad (12)$$

the quantity αA can be simplified using Eqs. (1) and (3):

$$\begin{aligned} t &= \frac{p}{2} \frac{p}{n\pi\langle R^2 \rangle} \\ &= \frac{p}{2} \lambda \end{aligned} \quad (13)$$

Therefore, at low air contents the Attiogbe equation t is approximately equal to one half the mean free path between air voids in a paste-air system.

4.5 Pleau and Pigeon Spacing Equation

Pleau and Pigeon [6] have recently proposed a spacing equation for the paste-void spacing distribution. Their approach considered both the air void radii distribution and the distribution of distances between a random point in the paste and the nearest air void center. Let $h(x)$ represent the probability density function of the distance between a random point in the system and the center of the nearest air void. As defined before, let $f(r)$ represent the probability density function of air void radii. The joint probability [16] that this random point is a distance s from the surface of an air void with radius r is

$$\beta(s, r) = h(r + s)f(r) \quad (14)$$

As an approximation for $h(x)$, Pleau and Pigeon use the probability density function for the nearest neighbor distance between random points,

$$h(x) = 4\pi n e^{-\frac{4}{3}\pi n x^3} \quad (15)$$

which is attributable to Hertz [18]. However, the centers of air voids are not entirely random since air voids do not overlap one another. The consequence of this choice for $h(x)$ is discussed subsequently.

The joint probability density function $\beta(s, r)$ depends upon $h(s + r)$. If a point chosen at random throughout the entire system lies at a distance x from the center of a sphere, the quantity s is defined as $x - r$. Therefore, if the random point lies within the sphere, the quantity s will be negative, but the argument x of $h(x)$ will be either zero or some positive number.

The parameter r may be eliminated from the joint probability $\beta(s, r)$ by integrating over the possible radii,

$$k(s) = \int_0^\infty h(r + s) f(r) \Theta(r + s) dr \quad (16)$$

where the Heaviside function $\Theta(r + s)$ [20] insures that the argument of the function h remains positive. This equation is the fundamental equation of Pleau and Pigeon. The cumulative distribution function is

$$K'(s) = \int_{-\infty}^s k(s') ds' \quad (17)$$

and corresponds to the volume fraction of the entire system within s of an air void center. The volume fraction of the entire system that would lie within an air void is $K'(0)$, and corresponds to an estimate of the air void volume fraction. The volume fraction of paste within s of an air void surface would then be

$$K(s) = \frac{1}{Q} \int_0^s k(s') ds' \quad (18)$$

where Q normalizes the result by the volume fraction of paste.

The normalization factor Q should equal $1 - A$, or the paste volume fraction. By the authors' development, this is equivalent to

$$Q = 1 - K'(0) \tag{19}$$

which the authors use in their derivation. However, as demonstrated previously [21], for monosized spheres the quantity $K'(0)$ corresponds to the air volume fraction for a system of overlapping spheres. This is a consequence of using the Hertz distribution for $h(x)$.

In the subsequent numerical experiment, two results will be reported for the Pleau and Pigeon equation corresponding to the normalization factors $1 - K'(0)$ and $1 - A$.

4.6 Lu and Torquato Equations

The paste-void and the void-void spacing distributions have application both inside the the field of cementitious materials [22–27] and outside the field [28–30]. Using various approximation techniques, the problems of the paste-void and the void-void spacing distributions have been solved for systems composed of mono-sized spheres [31–37]. These approximations have been compared to results of Monte Carlo simulations [34, 35] and they are in agreement. One method of approximation relies upon n -point correlation functions, and Torquato, Lu, and Rubenstein [34] have obtained exact expansions for mono-sized spheres. Lu and Torquato [38] developed a means to map these correlation functions to systems of poly-dispersed sphere radii, thereby making it possible to extend the approximations for mono-sized spheres. These approximations for poly-dispersed sphere radii are given in Lu and Torquato [39], and are used here as estimates for both the paste-void and the void-void spacing distribution.

The results of Lu and Torquato [39] for both the paste-void and the void-void

proximity calculations require the following defined quantities:

$$\xi_k = \frac{\pi}{3} n 2^{k-1} \langle R^k \rangle \quad (20)$$

$$c = \frac{4 \langle R^2 \rangle}{1 - A} \quad (21)$$

$$d = \frac{4 \langle R \rangle}{1 - A} + \frac{12 \xi_2}{(1 - \xi_3)^2} \langle R^2 \rangle \quad (22)$$

$$g = \frac{4}{3(1 - A)} + \frac{8 \xi_2}{(1 - A)^2} \langle R \rangle + \frac{16}{3} \frac{B \xi_2^2}{(1 - A)^3} \langle R^3 \rangle \quad (23)$$

The value of B depends upon the exact way the system is constructed. For the calculations performed here, $B = 0$. Also, there was an error in the published value for g [39], which has been corrected here.

Since Lu and Torquato were studying systems composed of a matrix containing solid spheres they use the terms “void” and “particle” to represent the matrix and the spheres, respectively. Therefore, the authors’ “void exclusion probability” is used here to estimate the paste-void proximity distribution, and their “particle exclusion probability” is used here to estimate the void-void proximity distribution.

4.6.1 Paste-Void Proximity Distribution

The approach of Lu and Torquato [39] was to derive the probability that a point chosen at random

with $s < 0$ corresponding to the sphere of radius $-s$ being entirely inside an air void. The averaged quantity in Eqn. 24 has the same definition as before:

$$\langle (s+r)^3 \Theta(s+r) \rangle = \int_0^\infty (s+R)^3 \Theta(s+r) f(r) dr \quad (25)$$

Again, the quantity $\Theta(s+r)$ is the Heaviside step function [20], and insures that the argument $(s+r)$ remains positive.

This result can be recast into the air void problem. Since $e_v(s)$ represents the probability of a random point not being within a distance s of an air void surface, the probability of finding the nearest void surface within a distance s of a randomly chosen point is the complement of the void exclusion probability:

$$E'_v(s) = 1 - e_v(s) \quad (26)$$

The probability of finding the nearest air void surface a distance s from a random point in the paste portion only is

$$\begin{aligned} E_v(s) &= \frac{E'_v(s > 0) - A}{1 - A} \\ &= 1 - \exp \left[-\pi n (cs + ds^2 + gs^3) \right] \end{aligned} \quad (27)$$

This gives the fraction of the paste volume within a distance s of an air void surface, which is equivalent to the definition of the paste-void proximity cumulative distribution function.

4.6.2 Void-Void Proximity Distribution

The approach used by Lu and Torquato [39] for the void-void proximity is similar to that for the paste-void proximity. Given that a point is located at the center of an air void with radius R , the probability that the nearest air void surface is further away

than w is [39]

$$e_{\text{p}}(w, R) = \begin{cases} 1 & w \leq R \\ \exp \{ -\pi n [c(w - R) + d(w^2 - R^2) + g(w^3 - R^3)] \} & w > R \end{cases} \quad (28)$$

Lu and Torquato refer to this as the particle exclusion probability.

The probability that the nearest air void surface is within a distance w from the center of an air void with radius R is

$$E'_{\text{p}}(w, R) = 1 - e_{\text{p}}(w > R, R) \quad (29)$$

$$= 1 - \exp \left\{ -\pi n [c(w - R) + d(w^2 - R^2) + g(w^3 - R^3)] \right\} \quad (30)$$

Let s represent the shortest surface-surface distance between two air voids. The probability that the nearest air void surface is within s of the surface of the void with radius R is

$$E_{\text{p}}(s, R) = E'_{\text{p}}(s + R, R) \quad (31)$$

The function $E_{\text{p}}(s, R)$ is equivalent to the void-void spacing cumulative distribution function.

The most important feature of Eqn. 31 is that $E_{\text{p}}(s, R)$ depends upon the size of the sphere one starts from. For mono-dispersed sphere diameters, R is simply a constant. However, for a system composed of poly-dispersed sphere diameters, $E_{\text{p}}(s, R)$ is a continuous function of R . Since a continuous distribution of sphere diameters would have an infinite number of possible diameters, there would exist an infinite number of possible $E_{\text{p}}(s, R)$ distributions. This complicates an evaluation of void-void spacing distributions for systems composed of poly-dispersed sphere radii.

One possible remedy is to simply calculate an ensemble average. Ensemble averages can be calculated based on either number density or volume density. This bulk value can then be compared to measured values. Here, the number density ensemble average

was chosen:

$$\langle E_p(s) \rangle = \int_0^\infty E_p(s, r) f(r) dr \quad (32)$$

For a system of poly-dispersed sphere diameters one can also calculate the mean nearest surface-surface distance [39]:

$$l_p(R) = \int_R^\infty e_p(w, R) dw \quad (33)$$

which gives the average distance to the nearest air void surface when starting from spheres of radius R . The quantity $l_p(R)$ decreases as R increases. Therefore, on average, the larger the sphere one starts from, the shorter the distance one travels to reach the surface of the nearest air void. A technique is described to measure this quantity, and the results are given along with this prediction.

5 Numerical Experiment

The computer program used in this experiment was based upon one that was used previously in a similar experiment [41]. The computer generates sphere radii and sorts them in order of decreasing radii. Random locations are generated for the centers of the spheres, and they are placed inside a cube 10 mm long on a side. As the spheres are placed, should a new sphere overlap an existing one, new random locations for the center are generated until it no longer overlaps an existing sphere. This “parking” approach is used until all the spheres are placed into the cube. For any portion of a sphere protruding out from one face of the cube, there is a virtual sphere of the same size placed outside the opposite face such that its intruding portion exactly compensates for the protruding portion of the original sphere. This is the technique of periodic boundary conditions and helps to eliminate finite-size effects. Once all the spheres have been placed, the computer knows the size and location of every sphere in the system. From this, the computer can calculate any desired measure of spacing.

5.1 Air Void Radii Distribution

Two sphere radii distributions are used in this experiment: mono-sized and lognormally distributed radii. The mono-sized sphere systems provide a means to test the effects of varying either the size or the number density of air voids. The zeroth-order logarithmic radius distribution [40]

$$f(r) = \frac{\exp\left[-\frac{(\ln(r/r_o))^2}{2\sigma_o^2}\right]}{\sqrt{2\pi}\sigma_o r_o \exp(\sigma_o^2/2)} \quad (34)$$

represents an air void radii distribution typically found in concrete containing air entrainment. For this distribution ($r_o = 15 \mu\text{m}$, $\sigma_o = 0.736$), the specific surface area is 30.0 mm^{-1} . A plot of this distribution, and the corresponding ASTM C 457 chord distribution, $\phi(z)$ [42], is shown in Fig. 4. In this plot, the air void distribution is shown as a diameter distribution, $f(d)$, rather than a radius distribution since sphere diameters are more directly comparable to the observed ASTM C 457 chord distribution.

5.2 Paste-Void Proximity

After the spheres have been parked into the system, 1000 points throughout the entire system are chosen along a regular cubic grid. The distance from an individual point on the grid to the nearest sphere surface is calculated; if the point lies within that sphere, the shortest distance to the surface is made negative. These 1000 distances are then sorted, from smallest to largest. The relative rank of these distances, as a function of this distance, is an estimate of the cumulative distribution function for all the paste-void spacings in the entire system.

Since the negative distances in this CDF correspond to points lying within an air void, the 50 *th* and 95 *th* percentiles of the paste-void proximity spacings for the paste fraction alone are calculated from the positive values in the list of distances.

5.3 Void-Void Proximity

Analyzing void-void spacings is more complicated than the paste-void spacing measurements. As pointed out by Lu and Torquato, the void-void spacing distribution is a function of both s and r . For a lognormal distribution of sphere radii there exists a unique void-void spacing distribution for each sphere in the system. Also, estimating the average void-void spacing is difficult since only one measurement exists for each sphere, and that exact sphere diameter will not be duplicated in the system. An indirect means to estimating the average void-void spacing is presented and used here.

5.3.1 Ensemble Average Over All Particle Radii

The percentiles of the void-void spacing distribution are calculated in the same manner for both the mono-sized and lognormally distributed sphere radii. 1000 spheres are chosen at regular intervals from the sorted list of sphere radii which were used to place the spheres. For mono-sized spheres, this constitutes 1000 random air voids. For the lognormally distributed radii, this is a statistical ensemble based on the number density. For each of these 1000 spheres, the surface-surface distance to the nearest air void surface is calculated. This collection of distances is an estimate of the averaged distribution given in Eqn. 32. Once sorted in ascending order, the 500 *th* and 950 *th* entries correspond to the 50 *th* and 95 *th* percentiles of the void-void spacing distribution, respectively.

5.3.2 Mean Nearest Surface As A Function Of Particle Radius

The mean nearest surface for poly-dispersed sphere radii, $l_P(r)$, can be estimated from multiple iterations of void-void spacing measurements. As described in the previous section, 1000 spheres are chosen at regular intervals from the original sorted list of sphere radii. This list also corresponds to the cumulative distribution function of the sphere radii. If the void-void measurements are repeated from many system iterations, averaging the radii in the 500 *th* entry, for example, will yield an unbiased estimate of the 50 *th* percentile of the sphere radii distribution. Likewise, the corresponding nearest

sphere surface distance in the 500 *th* entry can be averaged, yielding an estimate of the mean nearest surface for the 50 *th* percentile.

This process is repeated for all 1000 entries of both sphere radii and void-void distances. Upon averaging over all system iterations, there are 1000 averaged radii and 1000 averaged void-void spacings. The 1000 averaged void-void spacings plotted against the corresponding 1000 averaged radii represents an estimate of $l_P(r)$.

5.4 Particle Dynamics

Strictly speaking, the Lu and Torquato equations are meant for equilibrium systems in which the spheres are allowed to mix and interact before coming into some equilibrium state. The mixing does not alter the size distribution of the spheres, only the locations of the spheres. From this description, air voids in concrete should also exhibit statistics of an equilibrium system, although the effect of gravity and the presence of the aggregates may not be ignored.

This computer experiment uses a parking approach to the final placement of the air voids. Once placed, the spheres do not move, nor do they interact with one another. The spatial statistics of both an equilibrium and a parked system can be quantified using an n -point correlation function, as was used by Lu and Torquato [39]. Although the spatial statistics of an equilibrium system and a parked system differ, they are similar at low air contents. Therefore, if the results of the computer experiment for mono-sized parked spheres agree with the exact Lu and Torquato results for mono-sized spheres, the spatial statistics, over the range of air contents tested, must be sufficiently similar between the equilibrium and the parked systems that the results are indistinguishable. This would suggest that the results for parked lognormally distributed air void radii are also a valid approximation for an equilibrium distribution of air void radii.

5.5 Statistics

In order to convey uncertainty in the reported values, iterations of the experiments must be performed, yielding statistical means and estimated standard deviations. An iteration here requires discarding all previous information about sphere locations and sizes. A completely new list of sphere diameters is created, sorted, and randomly parked within the system. From this new system, the different measures of spacing are performed, and the results recorded. After this, the information about sphere locations and sizes is once again discarded, and a new iteration begins. A mean and an estimated standard deviation for each measure of spacing are calculated from the values found for each iteration, and reported in the results.

6 Results

The results of the experiment are divided between the results for the mono-sized and for the lognormally distributed air void radii. The results of the mono-sized spheres demonstrate the effects of changing the number and the size of the spheres independently. The results of the lognormally distributed spheres should be indicative of most concretes containing entrained air.

All measured values reported here are represented by their mean and estimated standard deviation from 100 system iterations. Three different spacing quantities are reported: the paste-void (pv) and the void-void (vv) spacing percentiles, and the ensemble average void-void ($\bar{v}v$) spacing. A suffix is added to pv and vv to represent the percentile.

6.1 Mono-sized Spheres

The results of the mono-sized sphere experiments are shown in Tables 2 and 3. In each table, the results are divided between constant number density (n) and constant sphere diameter experiments, with one pair of values in common for both. The constant

number density experiments have 20 voids per cubic millimeter. The first constant number density experiment consists of voids with zero diameter. This is equivalent to placing 20 points per cubic millimeter. Since each point has no volume, the air content is zero. However, both the paste-void and void-void spacing distributions are well-defined.

6.1.1 Powers

Since the Powers spacing equation is an estimate of some large percentile of the paste-void spacing distribution, it is only included in the measurements of the 95 *th* percentile in Table 2. It is purely coincidental that for mono-sized spheres, the Powers equation is a good approximation of the paste-void spacing 95 *th* percentile. Throughout the entire experiment, the error is never more than 22 % for the 95 *th* percentile.

6.1.2 Philleo

The results in Table 2 indicate that the Philleo equation can make a reasonable estimate of both the 50 *th* and the 95 *th* percentiles of the paste-void spacing distribution. The maximum error was 24 % for the 50 *th* percentile, and 53 % for the 95 *th* percentile.

6.1.3 Pleau and Pigeon

The results of the Pleau and Pigeon equations for mono-sized spheres are shown in Table 2. Even though the renormalization parameter $K'(0)$ was in error at a sphere volume fraction of 0.28, there was negligible difference in the performance of K_A and $K_{K'}$ in estimating the 50 *th* percentile, for which, at a volume fraction of 0.28, both equations are in error by nearly a factor of two. At the 95 *th* percentile, the equation $K_{K'}$, which uses the incorrect estimate of the air content, performs noticeably better than K_A , but is still in error by nearly a third at a volume fraction of 0.28.

6.1.4 Attiogbe

The performance of both Attiogbe spacing equations are shown in Table 3 and Table 4. Table 3 shows the estimates of the 50 *th* and 95 *th* percentiles of the void-void spacing distribution. Table 4 shows the estimates of the average minimum spacing between voids. It appears as though neither Attiogbe equation can accurately predict the 50 *th* percentile, the 95 *th* percentile, or the mean of the void-void spacing distribution. However, as expected, the Attiogbe equation t is consistently one half the mean free path (λ).

There are aspects of the adjusted equation t_G in the constant number density experiment that warrant attention. First, in Table 3 the estimated spacing using t_G at zero air is 0.0000, which is unreasonable. If, as Attiogbe has defined his spacing, this is the average minimum spacing, all the spheres must be touching one another since there can be no negative distances between voids. However, as described previously, at zero air content in this experiment the voids are simply point particles, and they cannot be touching one another. Second, in the same table the estimated spacing t_G *increases* with increasing air content, and then decreases sharply at paste air content of about 12%, which corresponds to a concrete air content of about 4%. An increase in an estimation of the average minimum spacing between bubbles, with increasing air content, is unphysical for identical air voids.

6.1.5 Lu and Torquato

As shown in Tables 2 to 4, the Lu and Torquato equations consistently estimate well the parameters of both the paste-void and the void-void distributions. The largest errors were 8 % in the paste-void percentiles, 7 % in the void-void percentiles, and 5 % in the mean spacing between air voids.

6.2 Lognormally Distributed Spheres

The results of the lognormally distributed sphere radii are shown in Tables 5 and 6. The average void-void spacing as a function of radius is shown in Figs. 5 and 6 along with the measured values.

6.2.1 Powers Equation

Again, the Powers equation is only compared to the measurements of the 95 *th* percentile of the paste-void spacing distribution. As in the case of mono-sized spheres, the Powers equation is directly proportional to the 95 *th* percentile. However, for this distribution of lognormally distributed sphere radii, the Powers equation is a constant factor of 1.5 larger than the 95 *th* percentile.

6.2.2 Philleo Equation

The performance of the Philleo equation for lognormally distributed sphere radii is better than that for the mono-sized sphere radii. The maximum errors are 16% and 7% for the 50 *th* and 95 *th* percentiles, respectively.

6.2.3 Pleau and Pigeon Equation

For lognormally distributed sphere radii, the Pleau and Pigeon normalization factor $K'(0)$ is in error by 58% at an air volume of nearly 20%. This error is reflected in the performance of K_A and $K_{K'}$. For the case of lognormally distributed sphere radii, the equation K_A , which uses the correct air content, performs better than $K_{K'}$. This is in contrast to the mono-sized sphere case. Also, for lognormally distributed sphere radii, the Pleau and Pigeon equation overestimates percentiles, where as the equation underestimates percentiles of the mono-sized sphere radii.

6.2.4 Attiogbe Equations

As in the case of mono-sized spheres, the Attiogbe equation does not appear to estimate any reported statistic of the void-void spacing distribution. In the data shown in Table 6, the Attiogbe equation t is an order of magnitude greater than both the 50 *th* and the 95 *th* percentiles. As the paste air fraction increases from 0.02 to 0.07, the value of t_G only decreases by 10 %, where as the measured values decrease by 50 %.

6.2.5 Lu and Torquato Equations

As an estimate of the 50 *th* and 95 *th* percentiles, the Lu and Torquato equation performs better for lognormally distributed sphere radii than for mono-sized spheres. For the lognormally distributed air void radii used here, the maximum associated errors are 2 % and 1 % for the 50 *th* and 95 *th* percentiles of the paste-void spacing distribution, respectively. The void-void spacing percentile estimates for the lognormally distributed sphere radii have approximately the same performance as for the mono-sized spheres.

In addition to estimating the percentiles of the void-void spacing distribution, the Lu and Torquato equation is used to estimate the average void-void spacing as a function of sphere radius. The results are shown in Figs. 5 and 6. The measured data (solid circles) are the average of 100 system iterations. As can be seen in the figures, the Lu and Torquato equation $l_P(r)$ is accurate for paste air contents of nearly 20 %.

6.3 Paste-Void Probability Density

A graphical performance comparison of the Philleo, the Pleau and Pigeon, and the Lu and Torquato estimates of the paste-void proximity probability density function is shown in Fig. 7. The sphere radii are lognormally distributed with a number density of 240 mm⁻³. The Philleo estimate terminates at s equals zero since it is already normalized for the fraction of paste within s of an air void surface. The Lu and Torquato estimate is virtually exact at the resolution of this experiment. The Philleo estimate is fairly accurate for s greater than zero, while that of Pleau and Pigeon

is noticeably in error. These qualitative differences are born out in the previously reported results.

7 Discussion

These results suggest that the Powers spacing factor approximates some large percentile of the paste-void spacing distribution, as it was intended. However, the exact percentile is unknown, and appears to vary with the air void radii distribution.

The Philleo equation performed much better for lognormally distributed sphere radii than for mono-sized sphere radii. It is not clear why this should be so. Philleo did not consider any air void radii distribution in the development of his equation.

Although the Pleau and Pigeon equation works well at very low air contents, the performance of the equation worsens with increasing air content, especially for the lognormally distributed sphere radii. This is a consequence of using the Hertz distribution for $h(x)$. It is interesting to note that, for lognormally distributed air void radii, although the Pleau and Pigeon equation is a function of the sphere radii distribution, it does not perform as well as the Philleo equation, which is independent of the sphere radii distribution.

The performance of the Attiogbe equations in estimating percentiles of the void-void spacing distribution was quite poor. The original equation t is completely disconnected from the void-void spacing distribution, which is expected since it is proportional to the mean free path. However, the relevance of the mean free path to freeze-thaw durability is questionable. The adjusted equation t_G has unphysical behavior for mono-sized spheres with constant number density and increasing void radius. For lognormally distributed sphere radii, it is clear that neither equation has any relevance to any reported statistic of the void-void spacing distribution.

There is one quantitative aspects of the equation t_G that warrants further discussion. The equation t_G has a maximum value of $16/\alpha$ as the number density n of air voids approaches zero. This suggests that there is a finite distance between air voids

when there are virtually no air voids present, which is completely unphysical.

The performance of the Lu and Torquato equation is, by far, the most accurate estimate for every statistic considered. Not only does it predict these statistics well, it also predicts the average void-void spacing as a function of radius for poly-dispersed sphere radii. It appears as though the Lu and Torquato equation is accurate to the level of precision required for investigations of air void spacing. These results also suggest that an air void distribution approximated by a collection of parked spheres has very similar spatial statistics to an equilibrium distribution of spheres, which has relevance to numerical tests of air void equations. It is also interesting to note that the Lu and Torquato equations do require information about the entire air void radii distribution. Rather, only the values $\langle R \rangle$, $\langle R^2 \rangle$, and $\langle R^3 \rangle$ are needed. This has significant importance for stereological practices [15].

8 Summary

A computer program can serve as an effective means to evaluate the mathematical performance of various spacing equations. The computer allows one to monitor both the size and location of every sphere in the system, for any air void radii distribution. This computerized approach helps to assure that the successful freeze-thaw prediction performance of an equation is due, in part, to the successful geometrical performance of the equation. Without this, one has no basis for correlating freeze-thaw performance with the prediction of an equation.

Four air void spacing equations were considered: Powers, Philleo, Pleau and Pigeon, and Attiogbe. In addition, an equation by Lu and Torquato which also estimates the same spacing characteristics was considered. For the lognormally distributed radii used, the Powers equation is within a factor of 1.5 of the 95 *th* percentile of the fraction of paste within an air void surface. The Philleo equation estimated the 50 *th* and

as well as the Philleo equation for lognormally distributed sphere radii. The original Attiogbe equation is approximately a factor of two less than the paste mean free path and an order of magnitude greater than the 95 *th* percentile of the void-void spacing distribution. The adjusted Attiogbe equation estimates an increasing spacing between mono-sized air voids as the number remains fixed and the diameter *increases*. This behavior makes this equation an unlikely candidate as a measure of air void spacing in concrete.

The Lu and Torquato equations performed quite well for both paste-void and void-void spacing distributions. Not only can their equations predict arbitrary statistics of both the paste-void and void-void spacing distributions, they also accurately predict the average void-void spacing as a function of void radius.

Due to the accuracy of the Lu and Torquato equation, it would appear as though additional spacing equations are not needed. The Powers equation can be tested further for various air void radii distributions and compared to the Lu and Torquato equation. If the Powers equation fails to consistently predict the same percentile of the paste-void spacing distribution, it could be replaced with either the Lu and Torquato equation or a simplified approximation. Regardless, as the material properties of concrete continue to change, effort must also address establishing an appropriate limit of allowable spacing in concrete.

Acknowledgements

This paper would not have existed had it not been for the encouragement and advice from a number of friends and colleagues. First drafts received thoughtful comments from Dr. Ken Hover (Cornell University) and from Dr. Kumar Natesaiyer (U.S. Gypsum) who also brought the work of Pleau and Pigeon to my attention. I also received encouragement from Dr. Edward Garboczi (NIST) who made me aware of the paper by Lu and Torquato. The author wishes to acknowledge the support from the High Performance Construction Materials Program of the Building and Fire Research

Laboratory.

References

- [1] H.L. Kennedy, The function of entrained air in concrete, *J. Am. Concr. Inst.* **14**, 529–542 (1943).
- [2] T.C. Powers, The air requirement of frost-resistant concrete, *Proc. Highway Res. Board* **29**, 184–202 (1949).
- [3] American Society for Testing and Materials, Standard Test Method for Microscopical Determination of Parameters of the Air-Void System in Hardened Concrete, Designation: C 457 - 90, Philadelphia, PA, 1995.
- [4] R.E. Philleo, A method for analyzing void distribution in air-entrained concrete, *Cem. Concr. Aggregates* **5**, 128–130 (1983).
- [5] E.K. Attiogbe, Mean spacing of air voids in hardened concrete, *ACI Mater. J.* **90**, 174–181 (1993).
- [6] R. Pleau and M. Pigeon, The use of the flow length concept to assess the efficiency of air entrainment with regards to frost durability: Part I - Description of the test method, *Cem. Concr. Aggregates* **18**, 19–29 (1996).
- [7] R. Pleau, M. Pigeon, J.L. Laurencot, and R. Gagné, The use of the flow length concept to assess the efficiency of air entrainment with regards to frost durability: Part II - Experimental results, *Cem. Concr. Aggregates* **18**, 30–41 (1996).
- [8] E.K. Attiogbe, Predicting freeze-thaw durability of concrete - A new approach, *ACI Mater. J.* **93**, 457–464 (1996).
- [9] J.J. Filliben, DATAPLOT: Introduction and Overview, NBS Special Publication 667, National Institute of Standards and Technology, Gaithersburg, MD (1984).
- [10] C.F. Gerald and P.O. Wheatley, *Applied Numerical Analysis (Third Edition)*, Addison-Wesley, Reading (1984).
- [11] T.D. Larson, P.D. Cady, and J.J. Malloy, The protected paste volume concept using new air-void measurement and distribution tec

- [12] K. Natesaiyer, K.C. Hover, and K.A. Snyder, Protected-paste volume of air-entrained cement paste. Part I, *J. Mater. Civ. Eng.* **4**, 166–184 (1992).
- [13] K. Natesaiyer, K.C. Hover, and K.A. Snyder, Protected-paste volume of air-entrained cement paste. Part II, *J. Mater. Civ. Eng.* **5**, 170–186 (1993).
- [14] S. Diamond, S. Mindess, and J. Lovell, On the spacing between aggregate grains in concrete and the dimension of the aureole de transition, in *International RILEM Colloquium (Toulouse), Liaisons Pâtes de Ciment/Matériaux Associés, RILEM (1982) C42–C46*.
- [15] E.E. Underwood, *Quantitative Stereology*, Addison-Wesley, Reading (1970).
- [16] P.L. Meyer, *Introductory Probability and Statistical Applications (2nd Edition)*, Addison-Wesley, Reading (1970).
- [17] J. Marchand, R. Pleau, and R. Gagné, Deterioration of concrete due to freezing and thawing, *Materials Science of Concrete IV*, J. Skalny and S. Mindess, eds., The American Ceramics Society, Westerville, OH, (1995) 283–354.
- [18] P. Hertz, Über den gegenseitigen durchschnittlichen Abstand von Punkten, die mit bekannter mittlerer Dichte im Raume angeordnet sind, *Math. Ann.* **67**, 387–398 (1909).
- [19] K. Natesaiyer, M. Simon, and K. Snyder, Discussion of, ‘Mean spacing of air voids in hardened concrete’, *ACI Mater. J.* **91**, 123–124 (1994).
- [20] G. Arfken, *Mathematical Methods For Physicists*, Academic Press, New York (1970).
- [21] K.A. Snyder, Discussion of ‘The use of the flow length concept to assess the efficiency of air entrainment with regards to frost durability: Part I – Description of the test method’, *Cem. Concr. Aggregates* **19**, 116–119 (1997).
- [22] K.A. Snyder, D.N. Winslow, D.P. Bentz, and E.J. Garboczi, Effects of interfacial zone percolation on cement-based composite transport properties, in *Proceedings of the MRS, Vol. 245, Advanced Cementitious Systems: Mechanisms and Properties*, Materials Research Society, Pittsburgh (1992) 265–270.

- [23] K.A. Snyder, D.N. Winslow, D.P. Bentz, and E.J. Garboczi, Interfacial zone percolation in cement-aggregate composites, in Proceedings of the RILEM International Conference (Toulouse), Proceedings 18, Interfaces in Cementitious Composites, J.C. Maso, ed., E&FN Spon, London (1992) 259–268.
- [24] D.N. Winslow, M.D. Cohen, D.P. Bentz, K.A. Snyder, and E.J. Garboczi, Percolation and pore structure in mortars and concrete, *Cem. Concr. Res.* **24**, 25–37 (1994).
- [25] D.P. Bentz, J.T.G. Hwang, C. Hagwood, E.J. Garboczi, K.A. Snyder, N. Buenfeld, and K.L. Scrivener, Interfacial zone percolation in concrete: Effects of interfacial zone thickness and aggregate shape, in Proceedings of the MRS, Vol. 370, Microstructure of Cement-Based Systems: Bonding and Interfaces in Cementitious Materials, S. Diamond, S. Mindess, F. P. Glasser, L. W. Roberts, J. P. Skalny, and L. D. Wakele, eds., Materials Research Society, Pittsburgh (1994) 437–442.
- [26] E.J. Garboczi and D.P. Bentz, Analytical formulas for interfacial transition zone properties, *Adv. Cem. Based Mater.* **6**, 99–108 (1997).
- [27] E.J. Garboczi and D.P. Bentz, Multi-scale analytical/numerical theory of the diffusivity of concrete, (Submitted to) *Adv. Cem. Based Mater.*
- [28] S.B. Lee and S. Torquato, Porosity for the penetrable-concentric-shell model of two-phase disordered media: computer simulation results, *J. Chem. Phys.* **89**, 3258–3263 (1988).
- [29] J. Vieillard-Baron, Phase transitions of the classical hard-ellipse system, *J. Chem. Phys.* **56**, 4729–4744 (1972).
- [30] A.L.R. Bug, S.A. Safran, G.S. Grest, and I. Webman, Do interactions raise or lower a percolation threshold?, *Phys. Rev. Lett.* **55**, 1896–1899 (1985).
- [31] H. Reiss, H.L. Frisch, and J.L. Lebowitz, Statistical mechanics of rigid spheres, *J. Chem. Phys.* **31**, 369–380 (1959).

- [32] H. Reiss and R.V. Casberg, Radial distribution function for hard spheres from scaled particle theory, and an improved equation of state, *J. Chem. Phys.* **61**, 1107–1114 (1974).
- [33] J.R. MacDonald, On the mean separation of particles of finite size in one to three dimensions, *Mol. Phys.* **44**, 1043–1049 (1981).
- [34] S. Torquato, B. Lu, and J. Rubinstein, Nearest-neighbor distribution functions in many-body systems, *Phys. Rev. A* **41**, 2059–2075 (1990).
- [35] S. Torquato and S.B. Lee, Computer simulations of nearest-neighbor distribution functions and related quantities for hard-sphere systems, *Physica A* **167**, 361–383 (1990).
- [36] P.A. Rikvold and G. Stell, Porosity and specific surface for interpenetrable-sphere models of two-phase random media, *J. Chem. Phys.* **82**, 1014–1020 (1985).
- [37] P.A. Rikvold and G. Stell, D-dimension interpenetrable-sphere models of random two-phase media: Microstructure and an application to chromatography, *J. Coll. I. Sci.* **108**, 158–173 (1985).
- [38] B. Lu and S. Torquato, General formalism to characterize the microstructure of polydispersed random media, *Phys. Rev. A* **43**, 2078–2080 (1991).
- [39] B. Lu and S. Torquato, Nearest-surface distribution functions for polydispersed particle system, *Phys. Rev. A* **45**, 5530–5544 (1992).
- [40] W.F. Espenscheid, M. Kerker, and E. Matijević, Logarithmic distribution functions for colloidal particles, *J. Phys. Chem.* **68**, 3093–3097 (1964).
- [41] K.A. Snyder and J.R. Clifton, Measures of air void spacing, *Wiss. Z. Hochsch. Archit. Bauwes. (Weimar)* **40**, 155–157 (1994).
- [42] W.P. Reid, Distribution of sizes of spheres in a solid from a study of slices of the solid, *J. Math. Phys.* **34**, 95–102 (1955).

About the author: Kenneth A. Snyder is a physicist in the Building Materials Division of the NIST Building and Fire Research Laboratory. The National Institute of Standards and Technology is an agency of the Technology Administration, U.S. Department of Commerce.

Table 1: A sorted list of 20 random normal deviates x with mean zero and variance one, their rank, and their associated cumulative probability y .

x	Rank	y
-1.0730320	1	0.05
-0.8731335	2	0.10
-0.8409334	3	0.15
-0.7056352	4	0.20
-0.5254872	5	0.25
-0.4553703	6	0.30
-0.2430273	7	0.35
-0.1967312	8	0.40
-0.1494667	9	0.45
-0.1038428	10	0.50
0.0321516	11	0.55
0.0340721	12	0.60
0.2339296	13	0.65
0.2635231	14	0.70
0.2697059	15	0.75
0.4185625	16	0.80
0.5730767	17	0.85
0.8981169	18	0.90
1.1908520	19	0.95
1.5878820	20	1.00

Table 2: Estimates of the paste-void spacing percentiles for monosized spheres. The estimates include results from Pilleo (F); Pleau and Pigeon (K_A) and ($K_{K'}$) using the normalization factors of $1-A$ and $1-K'(0)$, respectively; Lu and Torquato (E_V); and Powers (\bar{L}). The measured values are labeled pv and have the one standard deviation uncertainties shown. The suffixes 50 and 95 indicate the percentile.

Diameter (mm)	n (mm ⁻³)	A	$K'(0)$	F50 (mm)	K_A 50 (mm)	$K_{K'}$ 50 (mm)	E_v 50 (mm)	pv50 (mm)
0.000	20	0.0000	0.0000	0.202	0.202	0.202	0.202	0.205 ± .006
0.025	20	0.0002	0.0002	0.190	0.190	0.190	0.190	0.191 ± .003
0.075	20	0.0044	0.0044	0.165	0.164	0.164	0.164	0.165 ± .003
0.150	20	0.035	0.035	0.130	0.124	0.124	0.125	0.124 ± .003
0.225	20	0.12	0.11	0.099	0.078	0.079	0.087	0.086 ± .003
0.300	20	0.28	0.25	0.072	0.024	0.028	0.053	0.052 ± .002
0.150	10	0.018	0.018	0.182	0.178	0.178	0.178	0.179 ± .003
0.150	20	0.035	0.035	0.130	0.124	0.124	0.125	0.124 ± .003
0.150	50	0.088	0.085	0.079	0.068	0.068	0.072	0.071 ± .002
0.150	100	0.18	0.16	0.051	0.033	0.034	0.042	0.041 ± .001

Diameter (mm)	n (mm ⁻³)	A	$K'(0)$	\bar{L} (mm)	F95 (mm)	K_A 95 (mm)	$K_{K'}$ 95 (mm)	E_v 95 (mm)	pv95 (mm)
0.000	20	0.0000	0.0000	0.320	0.330	0.330	0.330	0.330	0.330 ± .006
0.025	20	0.0002	0.0002	0.307	0.317	0.317	0.317	0.317	0.318 ± .005
0.075	20	0.0044	0.0044	0.282	0.292	0.289	0.289	0.290	0.292 ± .005
0.150	20	0.035	0.035	0.245	0.255	0.234	0.235	0.244	0.243 ± .005
0.225	20	0.12	0.11	0.207	0.219	0.166	0.168	0.190	0.186 ± .004
0.300	20	0.28	0.25	0.127	0.183	0.089	0.097	0.130	0.120 ± .003
0.150	10	0.018	0.018	0.328	0.341	0.326	0.326	0.333	0.335 ± .006
0.150	20	0.035	0.035	0.245	0.255	0.234	0.235	0.244	0.243 ± .005
0.150	50	0.088	0.085	0.161	0.169	0.138	0.139	0.152	0.149 ± .003
0.150	100	0.18	0.16	0.112	0.119	0.079	0.081	0.097	0.092 ± .002

Table 3: Estimates of the void-void spacing percentiles for monosized spheres. The estimates include results from Attiogbe (t) and (t_G); and Lu and Torquato (E_p). The measured quantities are labeled vv and have the one standard deviation uncertainties shown. The suffix 50 indicates the percentile.

Diameter (mm)	n (mm ⁻³)	A	t (mm)	t_G (mm)	E_p 50 (mm)	vv50 (mm)
0.000	20	0.0000	∞	0.000	0.202	0.211±.004
0.025	20	0.0002	50.91	0.067	0.177	0.178±.003
0.075	20	0.0044	5.609	0.198	0.130	0.130±.003
0.150	20	0.035	1.316	0.372	0.072	0.072±.002
0.225	20	0.12	0.488	0.465	0.034	0.036±.001
0.300	20	0.28	0.182	0.182	0.013	0.014±.001
0.150	10	0.018	2.730	0.386	0.117	0.118±.003
0.150	20	0.035	1.316	0.372	0.072	0.072±.002
0.150	50	0.088	0.470	0.332	0.032	0.033±.001
0.150	100	0.18	0.192	0.192	0.014	0.015±.001

Diameter (mm)	n (mm ⁻³)	A	t (mm)	t_G (mm)	E_p 95 (mm)	vv95 (mm)
0.000	20	0.0000	∞	0.000	0.330	0.378±.007
0.025	20	0.0002	50.91	0.067	0.304	0.320±.006
0.075	20	0.0044	5.609	0.198	0.254	0.260±.006
0.150	20	0.035	1.316	0.372	0.178	0.179±.005
0.225	20	0.12	0.488	0.465	0.107	0.109±.004
0.300	20	0.28	0.182	0.182	0.049	0.051±.002
0.150	10	0.018	2.730	0.386	0.264	0.269±.006
0.150	20	0.035	1.316	0.372	0.178	0.179±.005
0.150	50	0.088	0.470	0.332	0.093	0.094±.003
0.150	100	0.18	0.192	0.192	0.047	0.049±.002

Table 4: Estimates of the average void-void spacing and the mean free path (λ) for monosized spheres. The estimates include results from Attiogbe (t) and (t_G); and Lu and Torquato (l_P). The measured values are labeled $\bar{v}v$ and have the one standard deviation uncertainties shown.

Diameter (mm)	n (mm ⁻³)	A	λ (mm)	t (mm)	t_G (mm)	l_P (mm)	$\bar{v}v$ (mm)
0.000	20	0.0000	∞	∞	0.000	0.204	0.219 \pm .003
0.025	20	0.0002	101.84	50.91	0.067	0.179	0.183 \pm .002
0.075	20	0.0044	11.27	5.609	0.198	0.133	0.135 \pm .002
0.150	20	0.035	2.729	1.316	0.372	0.079	0.080 \pm .002
0.225	20	0.12	1.108	0.488	0.465	0.042	0.043 \pm .001
0.300	20	0.28	0.507	0.182	0.182	0.018	0.018 \pm .001
0.150	10	0.018	5.559	2.730	0.386	0.125	0.127 \pm .002
0.150	20	0.035	2.729	1.316	0.372	0.079	0.080 \pm .002
0.150	50	0.088	1.032	0.470	0.332	0.038	0.039 \pm .001
0.150	100	0.18	0.466	0.192	0.192	0.018	0.019 \pm .001

Table 5: Estimates of the paste-void distribution percentiles for lognormally distributed sphere radii. The estimates include results from Philleo (F); Pleau and Pigeon (K_A) and ($K_{K'}$) using the normalization factors of $1-A$ and $1-K'(0)$, respectively; Lu and Torquato (E_V); and Powers (\bar{L}). The measured values are labeled pv and have the one standard deviation uncertainties shown. The suffixes 50 and 95 indicate the percentile.

n (mm^{-3})	A	$K'(0)$	F50 (mm)	K_A 50 (mm)	$K_{K'}$ 50 (mm)	E_v 50 (mm)	pv50 (mm)
20	0.016	0.012	0.146	0.172	0.173	0.163	$0.162 \pm .003$
40	0.033	0.022	0.105	0.131	0.131	0.120	$0.120 \pm .002$
80	0.066	0.039	0.073	0.098	0.100	0.085	$0.085 \pm .002$
160	0.131	0.065	0.048	0.071	0.075	0.056	$0.057 \pm .002$
240	0.197	0.082	0.037	0.058	0.063	0.042	$0.043 \pm .001$

n (mm^{-3})	A	$K'(0)$	\bar{L} (mm)	F95 (mm)	K_A 95 (mm)	$K_{K'}$ 95 (mm)	E_v 95 (mm)	pv95 (mm)
20	0.016	0.012	0.450	0.272	0.302	0.304	0.290	$0.290 \pm .005$
40	0.033	0.022	0.337	0.204	0.231	0.236	0.220	$0.219 \pm .004$
80	0.066	0.039	0.247	0.150	0.173	0.185	0.162	$0.162 \pm .003$
160	0.131	0.065	0.175	0.108	0.125	0.143	0.114	$0.114 \pm .002$
240	0.197	0.082	0.136	0.087	0.099	0.123	0.089	$0.090 \pm .002$

Table 6: Estimates of the void-void distribution percentiles for lognormally distributed sphere radii. The estimates include results from Attiogbe (t) and (t_G); and Lu and Torquato (E_p). The measured values are labeled vv and have the one standard deviation uncertainties shown. The suffixes 50 and 95 indicate the percentile.

n (mm^{-3})	A	t (mm)	t_G (mm)	E_v 50 (mm)	vv50 (mm)
20	0.016	3.919	0.515	0.134	$0.134 \pm .003$
40	0.033	1.895	0.498	0.092	$0.093 \pm .002$
80	0.066	0.884	0.465	0.060	$0.060 \pm .002$
160	0.131	0.382	0.382	0.035	$0.035 \pm .001$
240	0.197	0.218	0.218	0.024	$0.024 \pm .001$

n (mm^{-3})	A	λ (mm)	t (mm)	t_G (mm)	E_v 95 (mm)	vv95 (mm)
20	0.016	7.969	3.919	0.515	0.263	$0.270 \pm .006$
40	0.033	3.918	1.895	0.498	0.194	$0.196 \pm .005$
80	0.066	1.892	0.884	0.465	0.138	$0.138 \pm .003$
160	0.131	0.880	0.382	0.382	0.092	$0.093 \pm .002$
240	0.197	0.542	0.218	0.218	0.069	$0.069 \pm .002$

Figure 1: An idealized representation of a spacing cumulative distribution function (CDF) and the associated probability density function (PDF) for some distance s . The dashed lines demonstrate how to determine the 50 *th* and the 95 *th* percentiles from CDF data.

Figure 2: The cumulative distribution function for the 20 normal random deviates shown in Table 1.

Figure 3: The cumulative distribution function (CDF) for the 1000 normal random deviates and the estimated probability density function (solid circles) for every 40 *th* deviate. The true gaussian probability density function is also given as a reference.

Figure 4: The zeroth-order logarithmic sphere diameter distribution $f(d)$, and the corresponding chord distribution $\phi(z)$, used in this experiment.

Figure 5: Mean void-void spacing (l_P) for lognormally distributed sphere radii with a density of 20 mm^{-3} . Measured values are shown as solid circles, the solid line is the estimate by Lu and Torquato.

Figure 6: Mean void-void spacing (l_P) for lognormally distributed sphere radii with a density of 240 mm^{-3} . Measured values are shown as solid circles, the solid line is the estimate by Lu and Torquato.

Figure 7: Estimates of the paste-void probability density function by Philleo, Pleau and Pigeon, and Lu and Torquato for lognormally distributed sphere radii with a number density of 240 mm^{-3} . Measured values are shown as filled circles.

Figure 1.

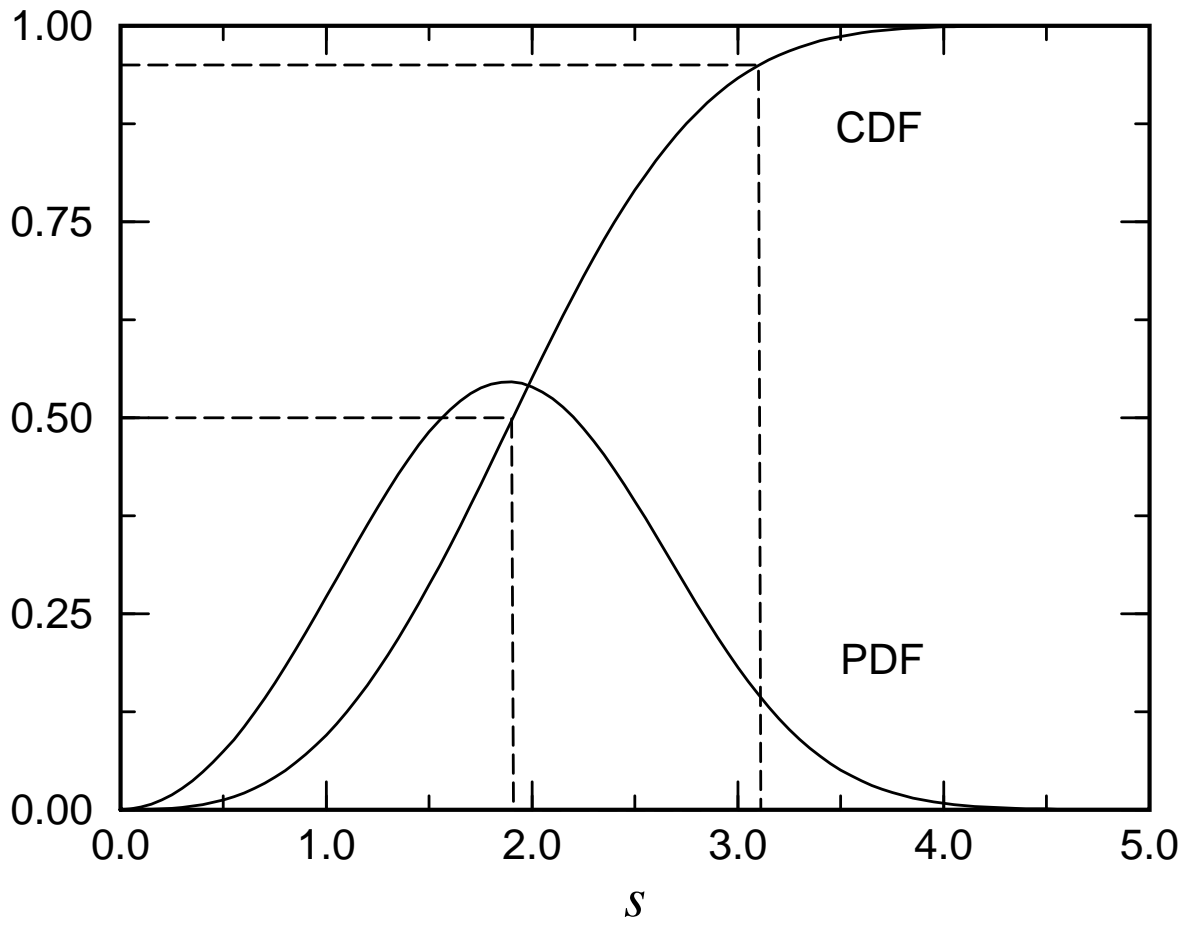


Figure 2.

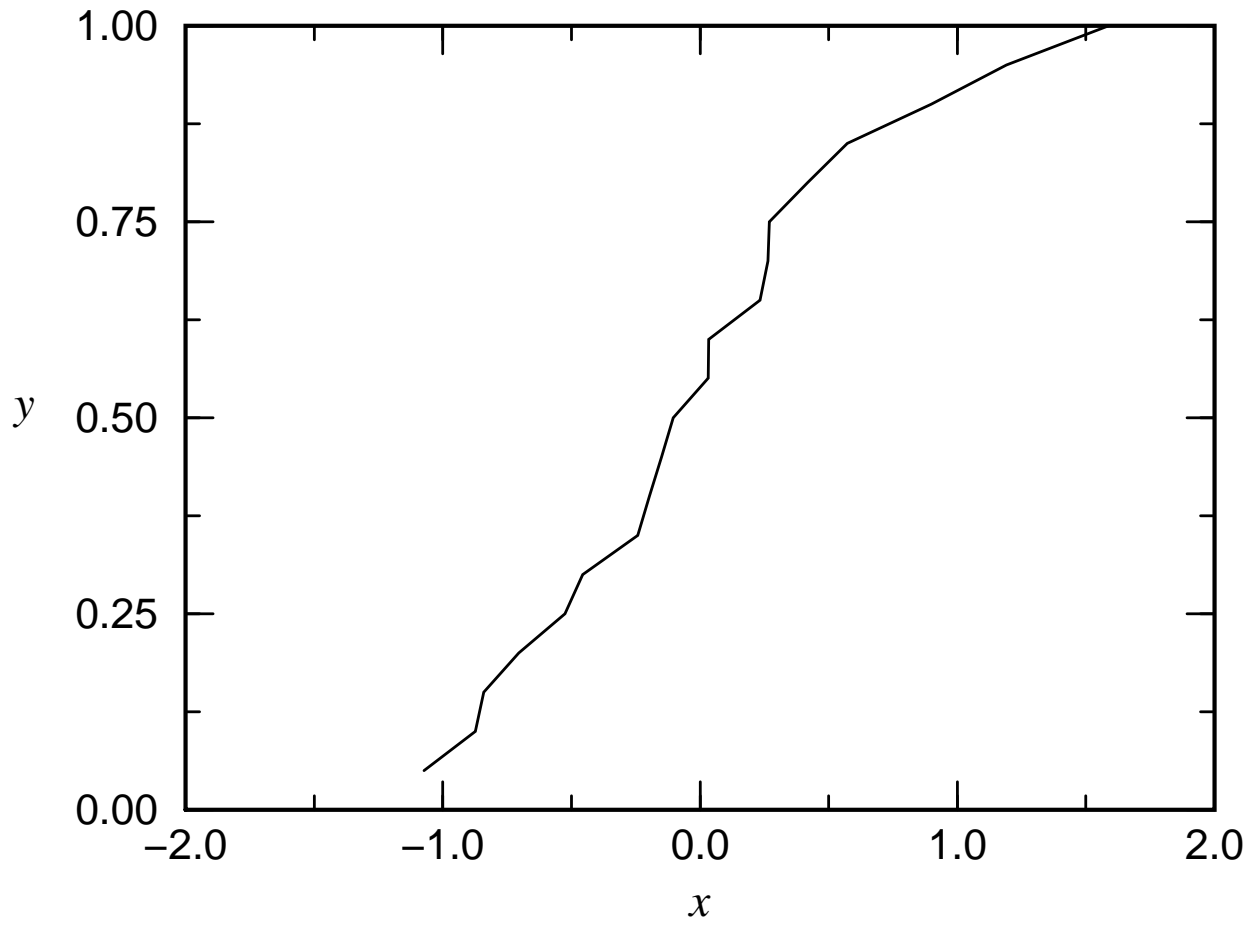


Figure 3.

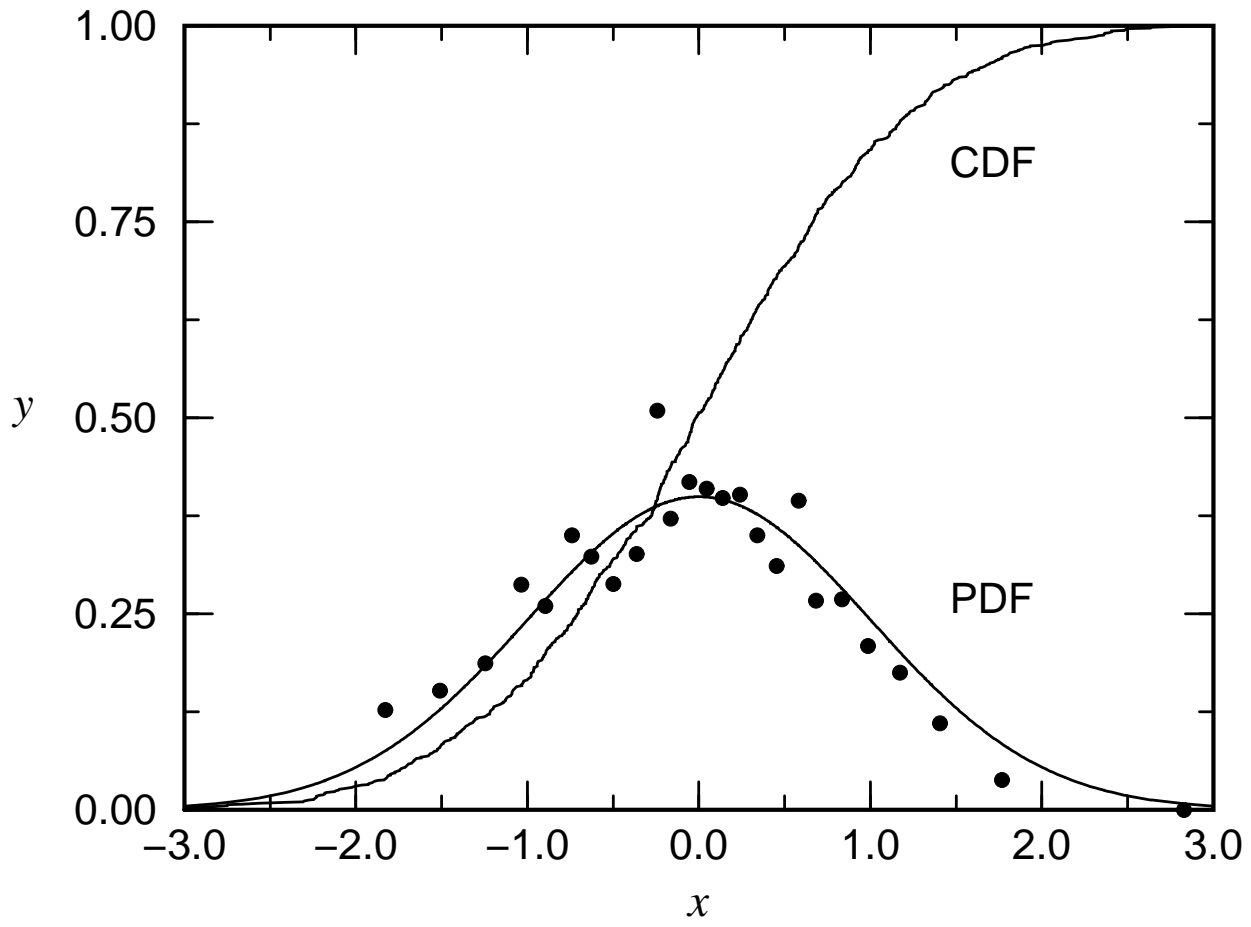


Figure 4.

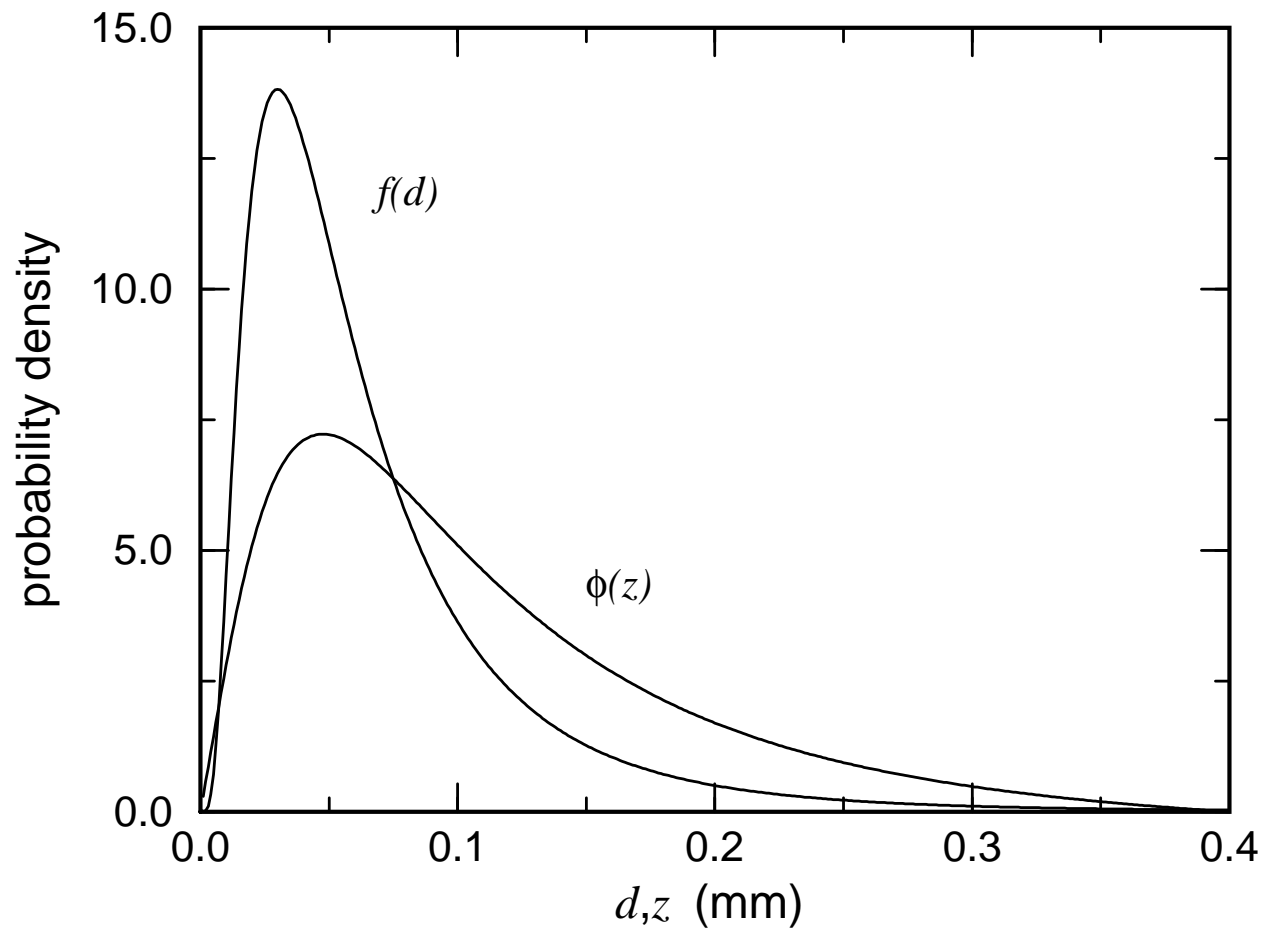
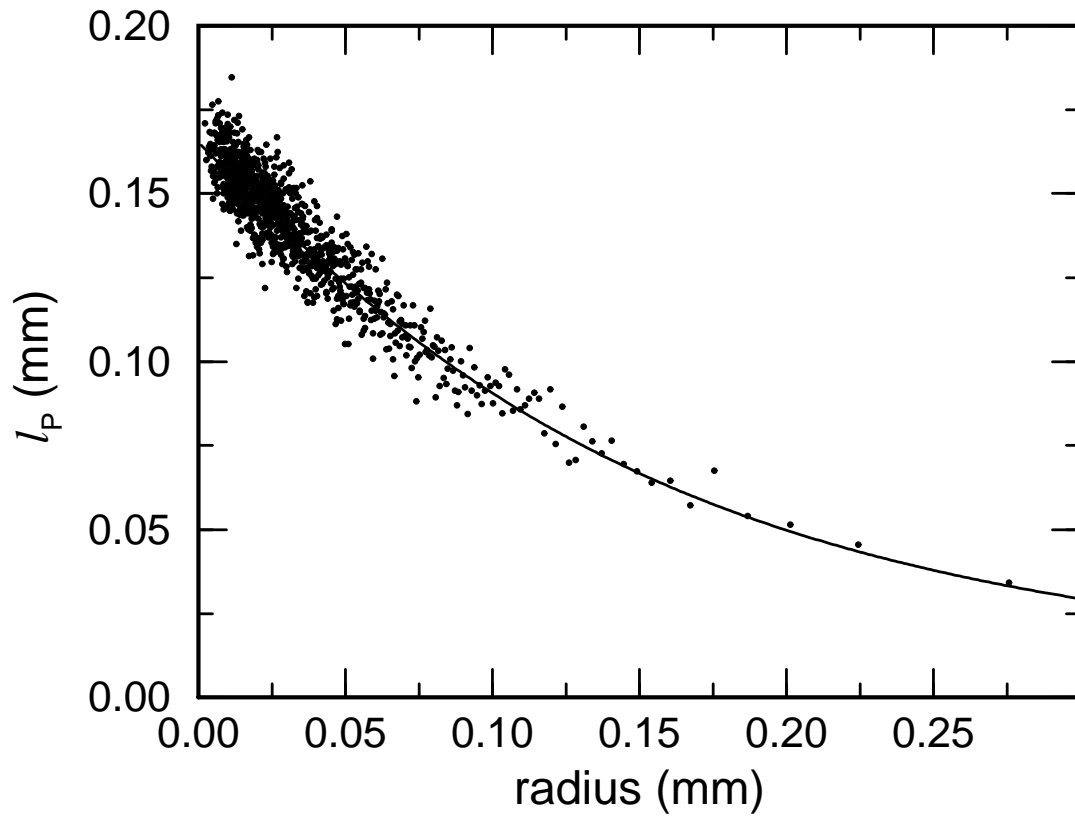


Figure 5.



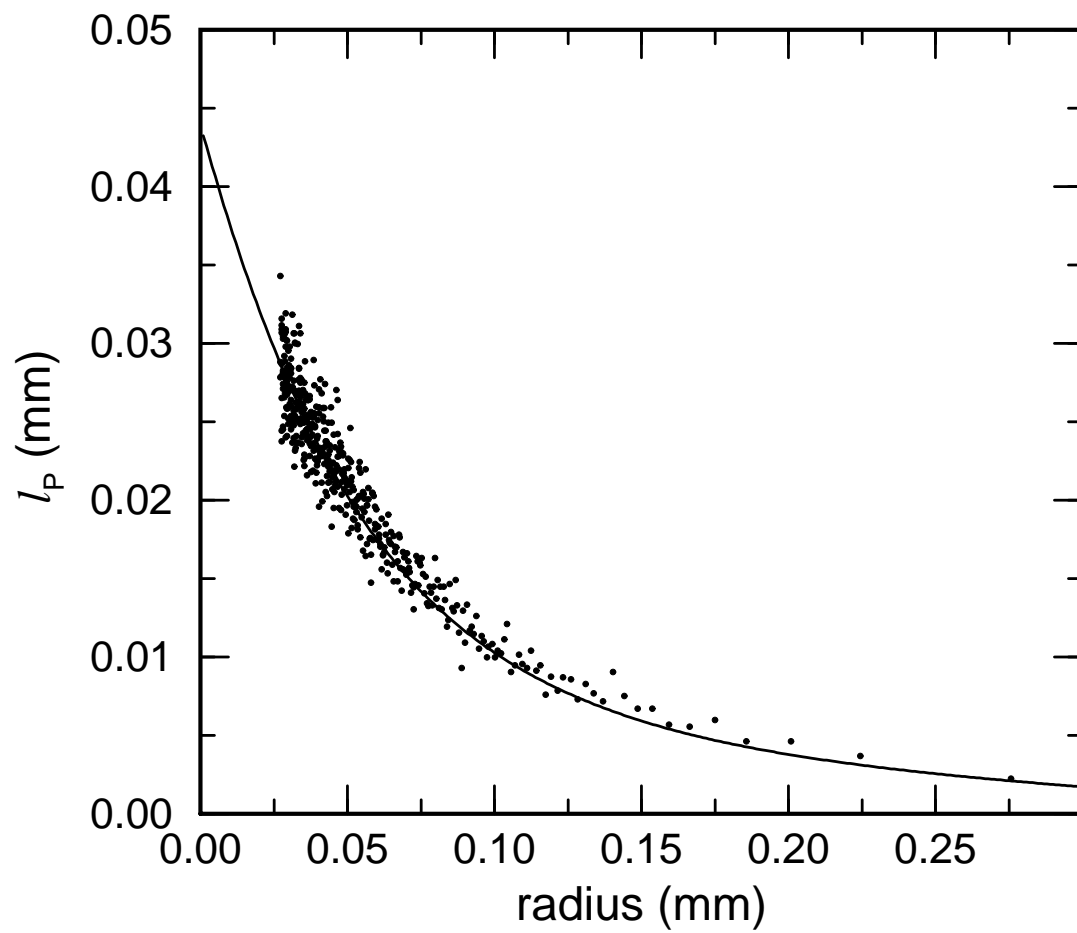


Figure 7.

